

A Voltage-Gated Ion Channel Based on a Bis-Macrocyclic Bolaamphiphile

T. M. Fyles,* D. Loock, and X. Zhou

Contribution from the Department of Chemistry, University of Victoria,
Victoria, British Columbia V8W 3P6, Canada

Received August 4, 1997

Abstract: The synthesis and characterization of a dissymmetric bis-macrocyclic bolaamphiphile ion channel is described. Bilayer-clamp experiments give rectified macroscopic current–voltage responses in which current is carried only at cis-negative potentials. Voltage and orientation-dependent irregular single-channel activity is also observed. Partial protonation of the carboxylate headgroups of the bolaamphiphile results in long-lived single channels with additional shorter-lived states of higher conductance. Single channels are also stabilized in the presence of barium cations. Vesicle experiments establish that transport activity is strongly cation- and concentration-dependent, suggesting the formation of aggregates. The voltage-gating process apparently involves the interaction of the applied potential with the molecular dipole of the bolaamphiphile which stabilizes an active aggregate.

The past decade has seen numerous designs for synthetic ion channels which promote ionic flux across bilayer membranes.^{1,2} To the extent that the designs have been tested, the basic requirements for artificial ion channels are relatively well-understood. Moreover, simple model systems have provided insights into natural systems: Fluxes approaching those exhibited by natural ion channels have been achieved,¹ the molecular origins of ion selectivity have been probed,³ and models have even suggested new roles for naturally occurring biopolymers.⁴ Despite the successes, current ion channel designs fall dramatically short of the performance of naturally occurring channels in the regulation of ionic flux.

Natural transporter proteins are highly regulated.⁵ The transition from a “closed” state to an “open”, or conducting, state typically requires a triggering stimulus: phosphorylation, small molecule binding (acetylcholine, Ca²⁺, etc.), or change in transmembrane potential.⁶ In contrast, most small molecule ion channels are effectively unregulated and shift to an open state due to random collisional activation processes within the

bilayer. The pentadecapeptide gramicidin is an excellent naturally occurring example,⁷ and many synthetic mimics are described as “gramicidin-like”.¹ An instructive exception is the nonadecapeptide alamethicin which is conductive only at positive transmembrane potentials above approximately 60 mV.^{7–9} The macroscopic current–voltage response is strongly rectified, making alamethicin a small-molecule model for voltage-gated channels such as the Na⁺ and K⁺ channels of nerve and muscle.⁵ The single-channel activity of alamethicin involves bursts of activity between several conducting states. Within a given conductance level, the single-channel current–voltage response is weakly voltage-dependent,⁸ but the magnitude of this inherent rectification is insufficient to account for the macroscopic current–voltage response.⁹ The mechanism of ion transport by alamethicin is relatively well-established: The peptide forms an amphipathic α -helix in the bilayer, and several of these helices associate to form active oligomeric bundles (“barrel-stave model”).^{7–9} There are several competing proposals for the origins of the voltage gating involving reorientation of the helices within the bilayer in response to the transmembrane potential.^{7–9}

A few synthetic voltage-gated ion channels are known. Peptides related to alamethicin^{8,10} and “minimalist” peptides designed to form ion channels by aggregation are weakly voltage-dependent.³ A nonpeptidic tetraalkylammonium butylene glycol phosphomonoester ion pair shows a range of voltage-gating behaviors which vary with each experiment.¹¹

* Send correspondence to this author at the University of Victoria. Telephone: (250) 721-7184. Fax: (250) 721-7147. E-mail: tmf@uvic.ca.

(1) The literature to late 1995 has been extensively reviewed: Gokel, G. W.; Murillo, O. *Acc. Chem. Res.* **1996**, *29*, 425–432. Fyles, T. M.; van Straaten-Nijenhuis, W. F. in *Comprehensive Supramolecular Chemistry*; Reinhoudt, D. N., Ed.; Elsevier Science Ltd.: Oxford, 1996; Vol. 10, pp 53–77. Voyer, N. *Top. Curr. Chem.* **1996**, *184*, 1–37.

(2) More recent examples reported: Wagner, H.; Harms, K.; Koert, U.; Meder, S.; Boheim, G. *Angew. Chem., Int. Ed. Engl.* **1996**, *35*, 2643–2646. Lein, L.; Jaikaran, D. C. J.; Zhang, Z.; Woolley, G. A. *J. Am. Chem. Soc.* **1996**, *118*, 12222–12223. Murillo, O.; Abel, E.; Maguire, G. E. M.; Gokel, G. W. *Chem. Commun.* **1996**, 2147–2148. Murillo, O.; Suzuki, I.; Abel, E.; Gokel, G. W. *J. Am. Chem. Soc.* **1996**, *118*, 7628–7629. Murillo, O.; Suzuki, I.; Abel, E.; Murray, C. L.; Meadows, E. S.; Jin, T.; Gokel, G. W. *J. Am. Chem. Soc.* **1997**, *119*, 5540–5549.

(3) Lear, J. D.; Schneider, J. P.; Kienker, P. K.; DeGrado, W. F. *J. Am. Chem. Soc.* **1997**, *119*, 3212–3217 and previous references to this peptide cited therein.

(4) Seebach, D.; Brunner, A.; Bürger, H. M.; Reusch, R. N.; Bramble, L. L. *Helv. Chim. Acta* **1996**, *79*, 507–517.

(5) Stein, W. *Carriers, Channels, and Pumps: An Introduction to Membrane Transport*; Academic Press: San Diego, 1990.

(6) Hille, B. *Ionic Channels of Excitable Membranes*; Sinauer Associates: Sunderland, 1984.

(7) Sansom, M. S. P. *Prog. Biophys. Mol. Biol.* **1991**, *55*, 139–235. Woolley, G. A.; Wallace, B. A. *J. Membr. Biol.* **1992**, *129*, 109–136. Cafiso, D. S. *Annu. Rev. Biophys. Biomol. Struct.* **1994**, *23*, 141–165.

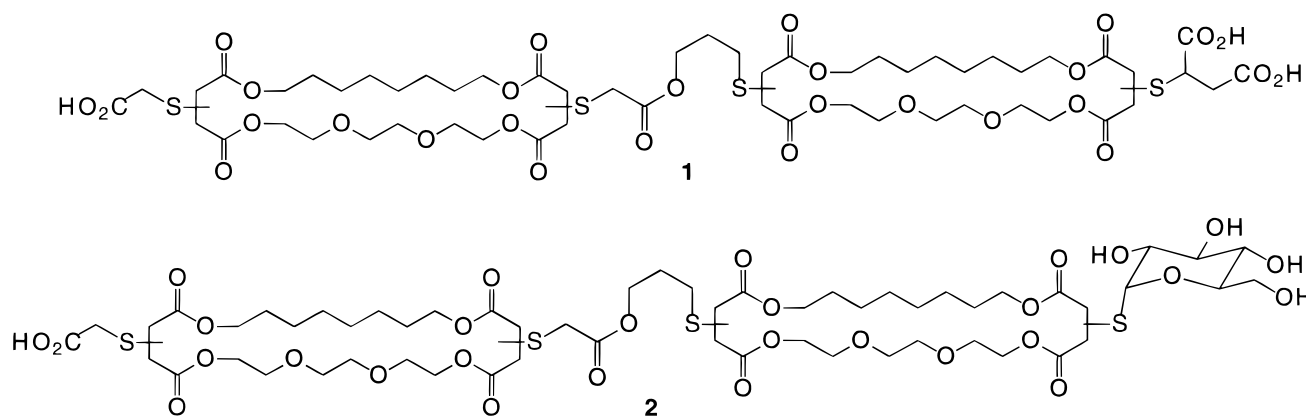
(8) Woolley, G. A.; Biggin, P. C.; Schultz, A.; Lien, L.; Jaikaran, D. C. J.; Breed, J.; Crowhurst, K.; Sansom, M. S. P. *Biophys. J.* **1997**, *73*, 770–778.

(9) Boheim, G.; Hanke, W.; Jung, G. *Biophys. Struct. Mech.* **1983**, *9*, 181–191.

(10) Woolley, G. A.; Epand, R. M.; Kerr, I. D.; Sansom, M. S. P.; Wallace, B. A. *Biochemistry* **1994**, *33*, 6850–6858. Matsubara, A.; Asami, A.; Akagi, A.; Nishino, A. *J. Chem. Soc., Chem. Commun.* **1996**, 2069–2070.

(11) Kobuke, Y.; Ueda, K.; Sokabe, M. *Chem. Lett.* **1995**, 435–436.

Chart 1



The discussions of all these systems invoke dipole reorientation in response to the applied potential as the origin of the voltage-gating response. A large molecular dipole is probably a necessary, but not a sufficient, condition since dipolar bis-macrocylic bolaamphiphiles show completely linear current–voltage responses.¹² Moreover, there is no evidence in the current–time conductance records of these derivatives to suggest any difference between parallel and antiparallel orientations of the bolaamphiphiles within an active aggregate (probably a dimer). We concluded previously that the bolaamphiphile headgroups (carboxylate, monosaccharide, and ammonium) could penetrate the bilayer so that both transmembrane orientations of molecules were formed.¹²

A voltage-gated channel is a desirable target, not only for the insights it might offer into the molecular nature of natural systems but also in its own right as a component of signal propagation, processing, or transduction devices.¹³ A voltage-gated channel is an ionic diode and, like macroscopic diodes, exhibits an asymmetric current response to an applied potential. The inherent asymmetry of the desired current–voltage response suggests that a degree of orientational asymmetry might be a good point of departure in the design of such a system. We reasoned that asymmetry could be imposed on the orientation of a bis-macrocylic bolaamphiphile by making one of the headgroups very hydrophilic. This would inhibit its transfer through the bilayer and would impose an asymmetric distribution in which the more hydrophilic headgroup would reside on the side of the membrane where the compound was added. There will be some limit to the size and charge of the hydrophilic headgroup as steric and electrostatic destabilization of active aggregates is anticipated. If, in addition, the molecule possessed a significant molecular dipole, then we might expect to observe voltage-gated channel activity. This could be manifested as a rectification of the single-channel conductance or, as for alamethicin, as a rectification of macroscopic ion currents due to many channels acting at once. This paper reports the synthesis of a suitable compound (**1**) and the evaluation of its performance as a voltage-gated ion channel.

Results and Discussion

Synthesis. Compound **1** was prepared by Michael addition of 2-mercaptosuccinic acid to the maleate precursor bis-macrocycle previously described.¹² As with analogous compounds in this series, it was isolated as a mixture of regio- and stereoisomers which behaved as a single component by analyti-

cal gel permeation chromatography and was fully characterized by NMR and MS (Chart 1).

Planar Bilayer Experiments. Voltage-gating behavior was examined using macroscopic ion currents induced by large numbers of channels formed by **1** in planar bilayers of diphytanoylphosphatidylcholine (diPhyPC) or a mixed lipid [egg phosphatidylcholine (PC)/egg phosphatidic acid (PA)/cholesterol (Chol), 8:1:1 mole ratio]. Sufficient **1** was added to the cis compartment of the bilayer clamp cell, and a voltage-ramp potential was applied (-100 to 100 mV at 6.3 mV s⁻¹). Figure 1A shows that significant current is carried only at negative applied potentials. The few cycles displayed in Figure 1A occur near the beginning of the experiment. Over a period of 10–15 min, the current asymmetry collapses so that current is carried at both negative and positive potentials. This is more clearly illustrated in the current–voltage diagrams given in Figure 1B; the average of the first seven voltage ramps shows a strongly rectified response, which is absent in the average response later in the experiment.

Alamethicin shows a similar time dependence in its current–voltage response. “Ideal” alamethicin-induced current occurs only at cis-positive potentials, while current carried at negative potentials at later times in an experiment is due to leakage of alamethicin through the bilayer.⁸ The current–voltage response of alamethicin under conditions similar to those of Figure 1 is given in Figure 2. In contrast, the previously reported analogue **2**¹² shows a symmetric current–voltage response (Figure 2).

The nearly linear current–voltage response of **2** was previously ascribed to a random transmembrane orientation of the thioacetate and thioglucose headgroups.¹² We conclude that the same must apply to **1** at late times in the experiment. At early times, **1** forms voltage-gated channels due to an asymmetric orientation within the bilayer, presumably with the succinate headgroups on the cis side of the bilayer. As the experiment progresses, succinate headgroups eventually penetrate the bilayer to produce both transmembrane orientations of **1**. If this picture is correct, then the sense of the voltage gating should depend on the side of the membrane to which **1** is added. Consistent with this prediction, addition of **1** to the trans compartment results in current rectification that is opposite of that illustrated in Figure 1 (current carried at cis-positive potentials). Only a linear (ohmic) current–voltage response is found if **1** is mixed with lipid before membrane formation.

Under “single-channel” conditions, compound **1** shows bursts of irregular openings (Figure 3A). The openings are brief, on the order of 0.5–10 ms, and the current carried in each opening ranges over 1 order of magnitude (1–10 pA). As shown in Figure 3A, the bursts appear to be clustered. Periods of

(12) Fyles, T. M.; Loock, D.; van Straaten-Nijenhuis, W. F.; Zhou, X. *J. Org. Chem.* **1996**, *61*, 8866–8874.

(13) Lehn, J.-L. *Angew. Chem., Int. Ed. Engl.* **1990**, *29*, 1304–1319.

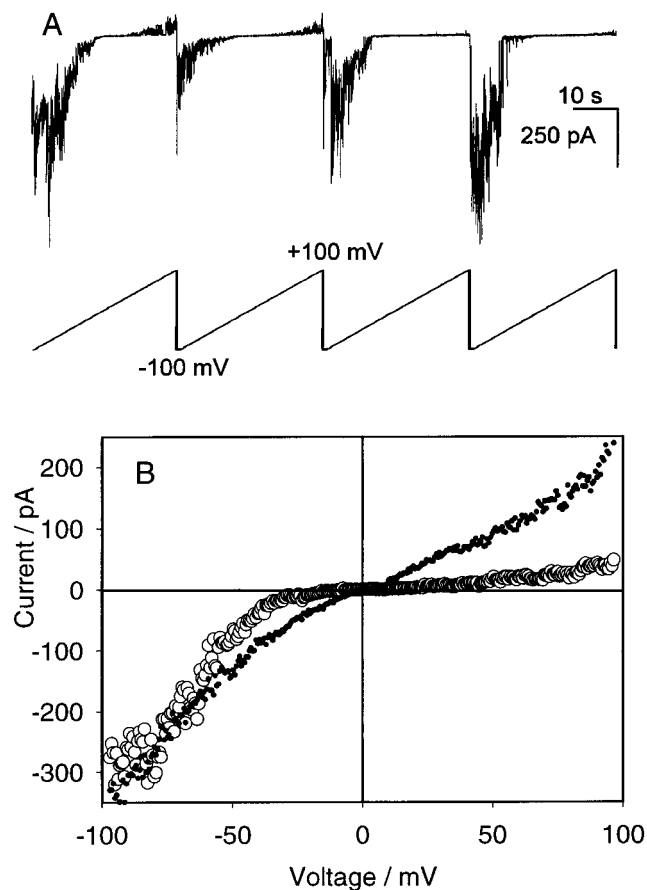


Figure 1. Macroscopic current–voltage relationships for **1**: (A) current as a function of time (upper trace) in response to varying applied potential (lower trace) early in an experiment (118 nmol of **1**; 1 M LiCl, diPhyPC) and (B) current averaged over cycles 1–7 (○) and 8–20 (●) as a function of applied potential for the experiment of A (data set reduced 1:50).

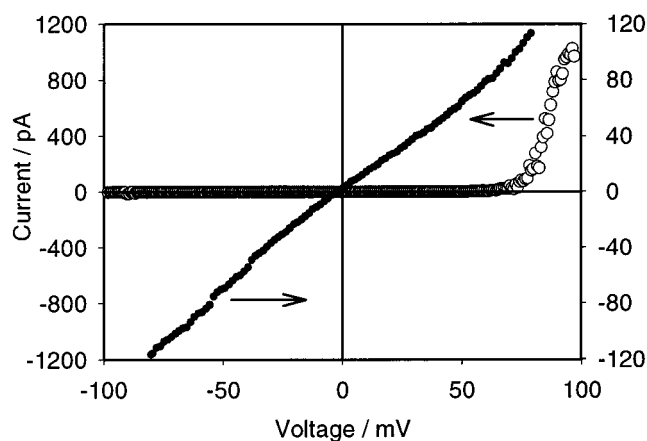


Figure 2. Average macroscopic current–voltage relationships for alamethicin (○, 130 pmol; 1 M KCl, PC/PA/Chol, 10 cycles from –100 to 100 mV at 5.7 mV s⁻¹, data set reduced 1:10) and **2** (●, 65 nmol; 1 M KCl, diPhyPC, 10 cycles from –100 to 100 mV at 4.8 mV s⁻¹, data set reduced 1:10).

quiescence are followed by periods of high activity which taper off. Figure 3 is representative of behavior which persists for periods of hours. This erratic behavior contrasts with the single-channel behavior of **2** and related derivatives,¹² which show regular step-conductance changes of long duration. The irregular behavior of **1** is not due to any asymmetry of orientation but is a property related to the succinate headgroup. Figure 3B shows the single-channel behavior of **1** mixed with lipid

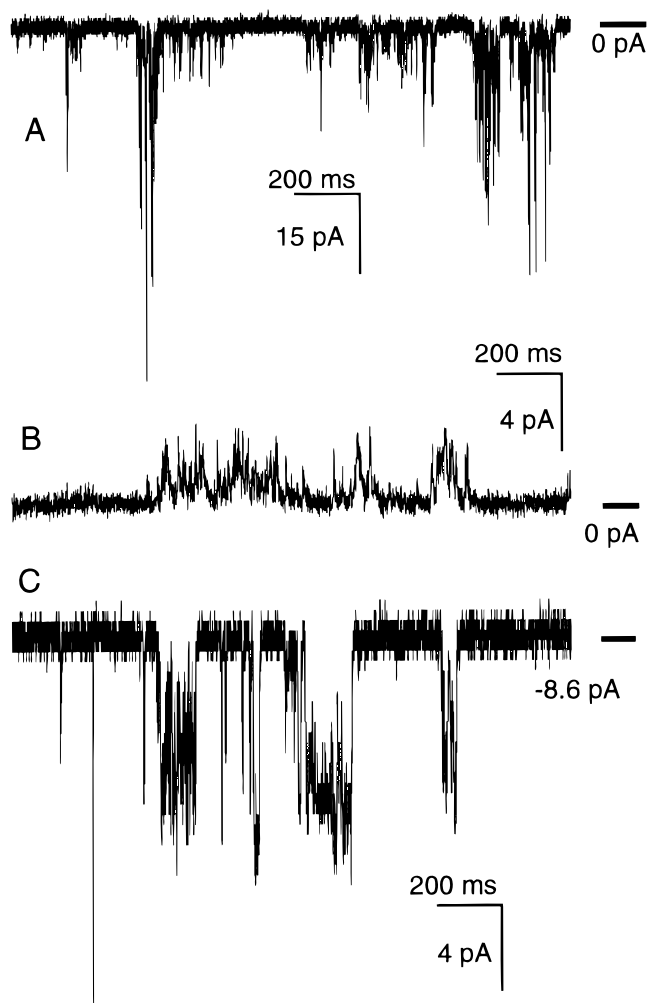


Figure 3. Current–time relationships for single channels of **1**: (A) 140 nmol of **1** added to the cis compartment (pH 6.4, 1 M KCl, diPhyPC, –120 mV), (B) 110 nmol of **1** mixed with 2.0 μmol of diPhyPC before bilayer formation (pH 6.4, 1 M KCl, 120 mV) (C) 200 nmol of **1** added to the cis compartment (pH 5.9, 1 M KCl, diPhyPC, –120 mV).

before membrane formation. As noted above, this procedure will result in both orientations of **1** and destroys the current rectification response. It does not produce regular well-behaved step-conductance changes. The excursions of current are dampened relative to Figure 3A, but bursts of short-lived and erratic openings are observed.

The shorter openings of **1** relative to those of **2** and related derivatives might be a consequence of electrostatic repulsions between dianionic succinate headgroups in an oriented aggregate. At the pH of the experiments of Figure 3A,B (6.4), the succinate headgroups will be approximately 15% monoprotonated and 85% fully deprotonated.¹⁴ We reasoned that at lower pH, further protonation of the succinate would occur to reduce the headgroup repulsions. The effect of a shift of pH to 5.9 is illustrated in Figure 3C. Under these conditions, the succinate headgroups are approximately 40% monoprotonated and 60% deprotonated. The main open state is an extremely long-lived pore (open lifetime being more than minutes) which carries a current of -8.65 ± 0.5 pA. This corresponds to a specific conductance of 72 ± 4 pS, approximately 5 times larger than the conductance exhibited by **2** and related compounds.¹² This long-lived state is interrupted by shorter-lived open states

(14) Assuming the succinic acid $pK_{a2} = 5.6$.

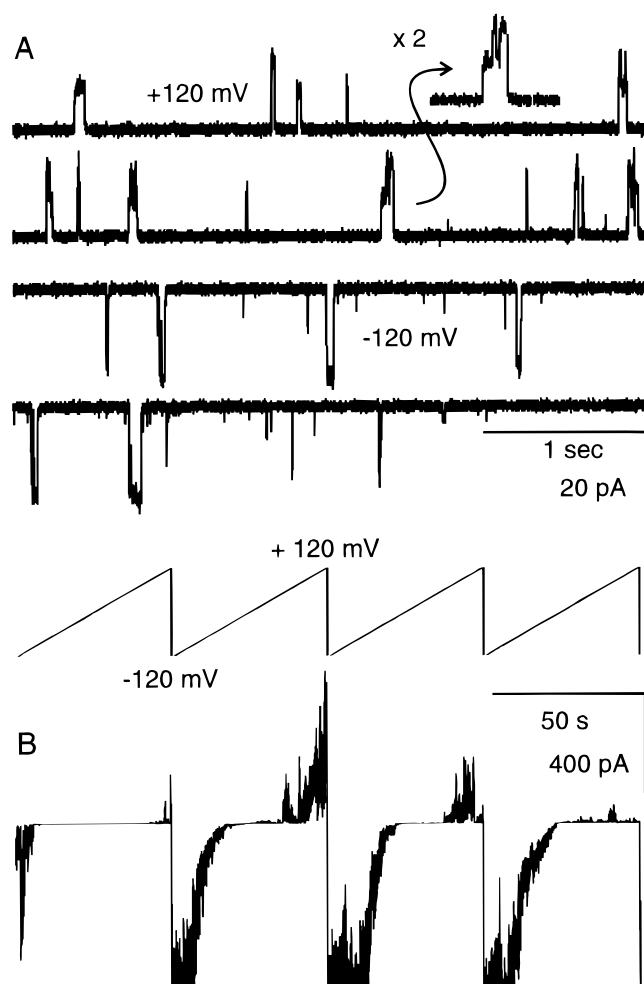


Figure 4. Conductance behavior of **1** in the presence of barium: (A) single channels at 120 mV (upper trace) and -120 mV (lower trace) and (B) macroscopic current as a function of time (lower trace) in response to varying applied potential (upper trace) (200 nmol of **1**, 1 M KCl, 1.6×10^{-3} M BaCl₂, voltage ramp at 4.7 mV/s).

carrying currents of -11 to -18 pA. Since these short-lived states are not direct conductance multiples of the long-lived open state, we interpret this as several different open states. These might be additional states of the long-lived channel or might be additional channels acting independently. The long-lived state shows a linear current–voltage relationship indicating that it is not inherently rectifying. This result cannot directly predict the properties of the shorter-lived channels at pH 6.4, since in addition to reducing the headgroup repulsions, the lower pH would be expected to promote penetration of the succinate headgroup through the bilayer, resulting in a random trans-membrane distribution of **1**.

Following similar logic, we reasoned that headgroup repulsions within an aggregate could be minimized by partial charge masking with divalent cations. That expectation was confirmed as illustrated in Figure 4 A, which shows that discrete single channels of **1** can be achieved in the presence of a low concentration of barium salts. In addition to some short-lived erratic events, well-defined step-conductance changes are observed. These have open lifetimes of 10–100 ms with clearly defined square-topped current amplitudes. These channels typically open one at a time, but occasionally show multiple openings typically observed with **2** and related derivatives (inset of Figure 4A).¹² The distribution of current amplitudes is broad, ranging from 8 to 25 pA per opening over a range of independent experiments. At negative applied potentials, the

experiment of Figure 4A gave 20.1 ± 3.1 pA for the main conductance state ($n = 108$) with a broad tail toward lower conductance. At positive potentials, the distribution was bimodal with clear maxima at 10.2 ± 2.1 and 16.7 ± 2.7 pA ($n = 97$). Two levels suggests the formation of aggregates with different numbers of monomers or different arrangements of the same number of monomers at positive potentials. The aggregates do not increase in size by addition of monomers during the open state, as is typical for alamethicin; thus, it is likely that the observed openings are initiated by the addition of a monomer to a nonconducting aggregate or by reorganization within a nonconducting aggregate. The difference in the illustrated experiment between positive and negative potentials is near the limit of significance, and the case for molecular scale rectification is not strong.

The macroscopic currents induced by these same channels of **1** in the presence of barium ions are partially rectified as illustrated in Figure 4B. The current response to the voltage ramp is initially strongly rectified. The second episode induces a nonrectified response which is attenuated in the third interval to regenerate a fully rectified response in the fourth interval illustrated. Rectification to nonrectification does not always cycle in the regular way given in Figure 4. Over a set of four independent experiments, roughly half of the cycles are highly rectified, as illustrated with cycles 1 and 4 ($n = 34$ cycles). The erratic rectification is conceivably due to an electrostatic stabilization of an active aggregate by barium ions which persists through to the opposite sign of the applied potential. In cases where this occurs, current is carried at positive potentials. In cases where the aggregates do not last as long, more complete rectification is observed. This effect would depend on the lifetime of the nonconducting precursor aggregate and would be expected to vary randomly as the openings themselves vary.

Outside of the “stabilized” conditions induced by pH changes or barium ions, is the voltage gating observed the result of a fixed number of channels which increase in size in response to the applied potential or the result of an increase in the number of active channels at a given potential? The irregular behavior of the single channels (Figure 3A) limits our ability to probe this question directly, but qualitative information is available from square-wave conductance change experiments (Figure 5). In Figure 5A, the potential is switched from -120 to 120 mV. Immediately following the first change, indicated by the large capacitive current, there is a delay of approximately 100 ms in which positive current is carried. A similar delay is evident at the onset of the second -120 mV segment. These delays occur in roughly 15% of the cases in five independent experiments ($n = 41$ cycles). This suggests a structured channel environment which can sometimes persist at the “wrong” potential and which sometimes takes time to form at the “right” potential. Note that, in the case of the first potential switch, the current carried at 120 mV is similar in magnitude (opposite in sign) to the current at -120 mV, indicating that the rectification involves ohmic channels as implied in the discussion of the pH- and barium-stabilized single channels. Figure 5B shows a smaller change in applied potential (-120 to -80 mV). Less current is carried at the less negative potential due to the smaller driving gradient. Even so, it is obvious that there are fewer openings at -80 mV, and fewer bursts of openings than found at -120 mV. A manual analysis suggests that there are about 20% of the number of “spikes” at -80 mV compared to those at -120 mV. Taken together, this qualitative analysis suggests that **1** is voltage-gated by virtue of larger numbers of open channels occurring at more negative potentials.

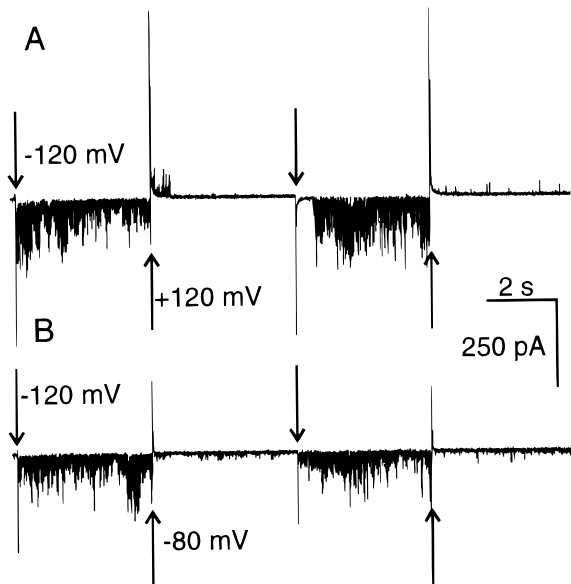


Figure 5. Macroscopic current–time relationships for multiple channels of **1** in response to a square-wave change in applied potential (200 nmol of **1**, pH 6.4, 1 M KCl): (A) 120/–120 mV, 0.5 Hz from points indicated; and (B) –120/–80 mV, 0.5 Hz from points indicated.

Implicit in the variety of conditions of electrolytes for Figures 1 and 3–5 is the fact that the pores formed by **1** are insensitive to the cation chosen for the electrolyte. This is not a surprising result given the high specific conductances which can be observed which suggest that large aqueous channels are formed. The pH and barium ion experiments clearly show the active channels are anionic; hence, some anion–cation selectivity would be expected. A dilution reversal potential of –31.4 mV was determined for a cell comprising 0.5 M KCl on the cis side and 0.1 M KCl on the trans side. According to the Goldman–Hodgkin–Katz equation,¹⁵ this corresponds to a K^+ : Cl^- selectivity of 14. This is similar in magnitude to the selectivity determined for **2**, but it is less selective than the related derivative with two thioacetate headgroups. This too is consistent with a larger channel being formed by **1** than by **2** and related compounds.

Vesicle Experiments. The transport activity of **1** in vesicles was examined using a pH-stat experiment,¹² in which transport is followed by monitoring the volume of titrant added to maintain a set pH in response to proton–cation antiport through a vesicle bilayer membrane. The conditions previously used (pH 6.6 internal solution, with the external pH set) establish a positive potential gradient relative to the external (cis) phase. We were unable to discover a lipid/buffer/vesicle preparation process which maintained a pH gradient in the opposite sense (outside acidic relative to inside) for a long enough time; hence, we were unable to carry out a pH-stat experiment equivalent to the voltage-gating experiment above.

Nonetheless, vesicle experiments provide some insights into the channels formed by **1**. Some results are summarized in Figure 6 which shows the extent of transport as a function of time after addition of **1** for a variety of conditions (cation, concentration of **1**). The most notable effect is the cation selectivity evident in the significant rate differences between Rb^+ (A), Cs^+ (B), and K^+ (C) (Na^+ and Li^+ not shown). These differences are 2–5 times greater than previously observed for related compounds yet are consistent with an effect noted previously whereby high anionic charge leads to increased cation

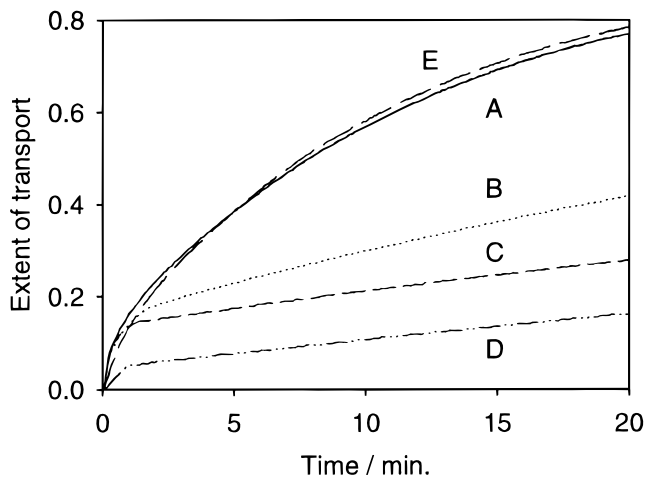


Figure 6. Extent of cation–proton antiport as a function of time as assessed by pH-stat titration of PC/PA/Chol vesicles (0.5 mM lipids): external electrolyte contained 0.02 M $RbCl$, (A, D, and E), 0.02 M $CsCl$ (B), or 0.02 M KCl , (C) and 21 μM **1** (A–C), 5.3 μM **1** (D), or 10.6 μM **1** (E).

selectivity.¹² The selectivity here follows the Eisenmann II sequence,¹⁵ indicating an electrostatic interaction between the hydrated cations and **1**. Compound **1** transporting Rb^+ at the maximum rate shows a ρ of specific activity comparable to that of the most active of the previously reported materials.¹² For transport of the other alkali metal cations, compound **1** is significantly less active than other compounds in this series, e.g. **2**. Thus, the Rb^+ cation selectivity has been achieved by retarding the other cations, not by accelerating the Rb^+ rate.

Figure 6 also shows a very marked dependence of transport on the concentration of **1**. At a concentration of 5.3 μM in **1** (curve D), a small initial disruption is followed by a slow transport rate near the lower limit for the experiment (0.9×10^{-10} mol of H^+ s^{-1}). Doubling the concentration to 10.6 μM results in a 16-fold increase in rate (curve E). Further concentration increases do not further accelerate transport.¹⁶ Thus, there is a very narrow window of concentration through which **1** shifts from virtually inactive to maximally active. The experimental uncertainties posed by this occurrence preclude a direct determination of the apparent kinetic order for **1**. It is certainly larger than 2–3 as found in related cases,¹² and certainly indicates that the channels formed by **1** involve aggregates.

Mechanism. Erratic openings of variable amplitude have no obvious parallel among well-behaved natural transporters. A referee has also pointed out that the amounts required for the activity are high relative to other active synthetic channels. Is it really appropriate to refer to the erratic behaviors illustrated above as being due to ion channels? We think so. Naturally occurring peptides such as melittin, the magainins, and the cecropins are described as “channel-forming”; however, all require significant concentrations in lipid for activity (1–5 mol %), and all typically exhibit “erratic” conductivity behaviors.¹⁸ The behavior of these peptides is also highly variable depending on lipid, concentration, and electrolyte. For **1**, the generally “high” levels needed to induce activity are quite variable. Note that the macroscopic multichannel currents in Figure 1 were induced with less **1** than the single-channel currents of Figure

(16) Zhou, X. Ph.D. Thesis, University of Victoria, Victoria, BC, 1997.

(17) Fyles, T. M.; Kaye, K. C.; Pryhitka, A.; Tweddell, J.; Zojaji, M. *Supramol. Chem.* 1994, 3, 197–209. Fyles, T. M.; James, T. D.; Kaye, K. C. *J. Am. Chem. Soc.* 1993, 115, 12315–12321.

(18) Bechinger, B. *J. Membr. Biol.* 1997, 156, 197–211.

(15) Eisenmann, G.; Horn, R. *J. Membr. Biol.* 1983, 197–225.

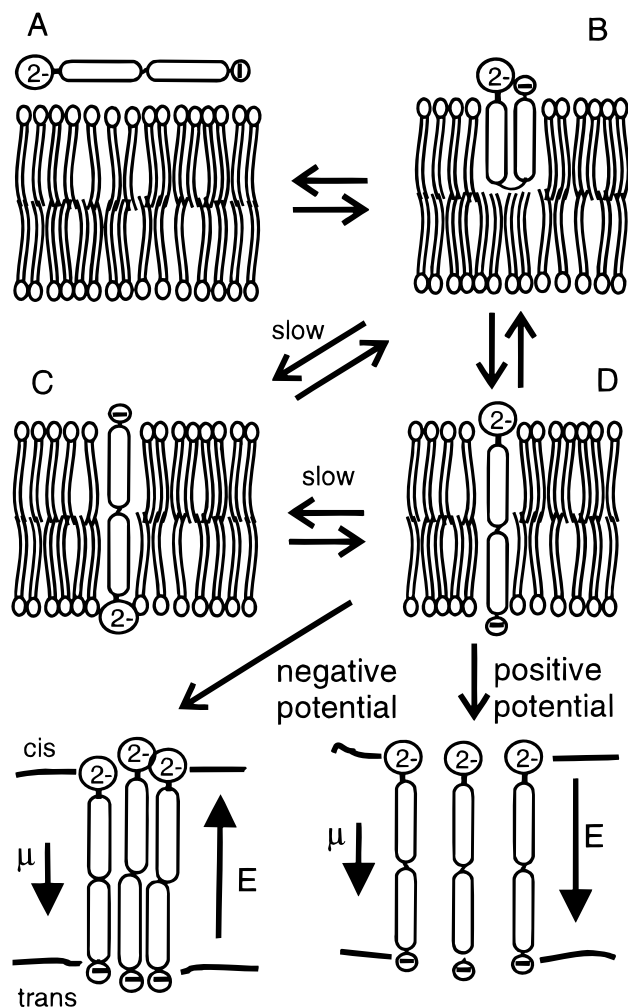


Figure 7. Proposed mechanism of voltage-dependent ion channel formation by **1**.

3A (118 vs 140 nmol, respectively). The data are also time-dependent, with a general increase in activity over periods of up to 1–2 h. This suggests that the partition of the transporter from the aqueous phase to the active bilayer is relatively slow and could be variable due to different positions of addition into the unstirred cell. Regular openings under the barium-stabilized conditions are similar to the openings induced by single molecule transporters; thus, it seems likely that relatively few of the many molecules added actually are observed. The exploration of synthetic ion transporters has greatly extended the range of structures which are considered as channels. We argue from the data presented here that “channel conductance behavior” should also include erratic events as well as the better characterized “square-topped” openings.

Given that **1** does form channels, our initial mechanistic assumption is that the channels formed by **1** are similar to those from **2** and its relatives.¹² The mechanism needs to account for the additional features of voltage gating and orientation-dependent openings, and high apparent kinetic order and cation selectivity from the vesicle experiment. A proposal is sketched in Figure 7. Beginning with a nonspecific association of **1** with the bilayer (A), a number of U-shaped (B) and transmembrane insertion states (C and D) can be envisaged. As shown previously, these must be electrically silent. Since the headgroup charges are unequal, the equilibria illustrated are dependent upon the sign of the applied potential. The processes involving penetration of the dianionic succinate headgroup through the membrane (B to C and D to C) are assumed to be

slower than the corresponding processes involving penetration of the monoanionic acetate headgroup (B to D). Thus, the first-formed transmembrane state achieved by a single molecule of **1** would be D, with the succinate headgroup on the cis face of the bilayer.

Application of a cis-negative potential to **1** oriented as in state D results in an antiparallel alignment of the molecular dipole of **1** and the electric field vector. This can be compared to the parallel arrangement of the molecular dipole and applied electric field under a cis-positive potential. The antiparallel arrangement is more stable, and an ion-conducting aggregate forms under a negative applied potential. Significant electrostatic repulsions between the succinate headgroups are expected, so the extent of aggregation will depend on the extent of stabilization afforded by the applied electric field. The parallel alignment of the dipole and electric field under cis-positive potentials is less stable at a given absolute value of applied potential; hence, electrostatic repulsions will dominate to a greater extent at positive potentials. This differential balance of forces results in the current rectification. In both cases, loosely structured aggregates are postulated. The difference between the negative and positive potential lies solely in the extent to which the aggregate can support a conducting channel. This occurs at a lower absolute magnitude of negative relative to positive potentials. This difference is sketched in Figure 7 as a closer approach of monomers under cis-negative potentials.

The marked cation selectivity of **1** in vesicles suggests that cation to headgroup interactions play an important role in the initiation of channels (under cis-positive potentials). Electrostatic interaction of the headgroups with counterions in solution will influence the aggregation, and this is the basis for the stabilization observed in the presence of added barium ions. All these observations point to the same conclusion; channel opening is a balance between headgroup repulsions and the orientation-dependent stabilization of the applied potential.

The aggregates which form under cis-negative potentials must be larger and more loosely structured than the active dimers proposed for **2** and related compounds. The higher apparent kinetic order is only one aspect. Other qualitative features (short burst openings, irregular amounts of current carried per opening, and lack of cation selectivity in the ion-translocation step) also suggest relatively poorly structured pores as the active species. The stable but not voltage-gated aggregate formed at pH 5.9 has a specific conductance substantially higher than that observed for **2**, indicating a much larger aqueous channel is formed by randomly oriented **1**. A referee asked whether such a long-lived opening has any relevance to biochemical ion transport. It probably does not, as a “wide open” aqueous pore would be difficult for any cell to accommodate. We note that this type of long-lived channel may have arisen at some point in the evolution of ion channels, but would not have survived to the modern era.

The voltage-gated pores formed by **1** suggest that the design of other types of controlled channels might be based on the stabilization and/or destabilization of ion-conducting aggregates. Aggregates stabilized by small-molecule binding by the headgroups would give rise to simple ligand-gated ion channels. Aggregates stabilized or destabilized by photoisomerization would give light-responsive switches. Our further explorations of this design motif will be reported in due course.

Experimental Section

Synthesis. General synthetic procedures and the preparation of **2** have been recently reported.¹²

3- or 4-[8'-[17''- or 18''-(2'''-Carboxy-1'''-thiaethyl)-1'',6'',9'',12'',15'',20''-hexaoxa-2'',5'',16'',19''-tetraoxocyclooctacos-3'- or 4'-yl]-6'-oxo-5',1',8'-oxadithiaoctyl]-17- or 18-(2-Carboxymethyl-3-carboxy-1-thiaproyl)-1,6,9,12,15,20-hexaoxa-2,5,16,19-tetraoxocyclooctacosane (1). A8TrgAP8Trg¹² (100 mg, 0.086 mmol) and 2-mercaptosuccinic acid (51 mg, 0.34 mmol, 4 equiv) were dissolved in tetrahydrofuran (15 mL), followed by addition of 2,2,6,6-tetramethylpiperidine (1.5 mL). The solution was refluxed for 6 h under nitrogen. After evaporation of the 2-propanol, the crude oil was dissolved in dichloromethane (200 mL), washed with 1 M hydrochloric acid (4 × 100 mL), and dried over sodium sulfate; the solvents were removed, and the yellowish mixture was chromatographed with a gel permeation column (LH-20, 3 × 60 cm) eluted with a solvent of 2-propanol/chloroform (3:4). The middle fractions were the compound expected on the basis of the results of the analytical GPC (Alltec, ID 10 × 250 mm) which gave a single sharp peak. The combined products were evaporated to give compound **1** as a pale yellow oil (100 mg, 0.076 mmol, 88%).

¹H NMR (360 MHz, CDCl₃): δ 7.37 (br s, 3H), 4.20 ~ 4.06 (m, 18H), 3.90 ~ 3.61 (m, 21H), 3.53 ~ 3.27 (m, 4H), 3.01 ~ 2.66 (m, 12H), 2.12 ~ 1.90 (m, 2H), 1.59 (br s, 8H), 1.28, 1.19 (br s, 16H).

¹³C NMR (90.57 MHz, CDCl₃): δ 173.4, 172.5, 171.1, 171.0, 170.2, 170.0, 169.6, 70.4, 70.2, 68.9, 68.8, 66.4, 65.8, 65.5, 65.0, 64.6, 64.3, 64.0, 63.9, 63.8, 42.4, 41.7, 36.7, 36.2, 35.9, 33.5, 33.1, 33.0, 29.6, 28.5, 28.2, 25.4, 25.2, 28.0, 27.9.

MS (LSIMS, mNBA): 1227.5 (M - HSCH₂CO₂H - H)⁻ 5.0%, 1319.5 (M - H)⁻ 100%. Exact mass: calcd for (M - H)⁻ (C₅₅H₈₃O₂₈S₄) *m/e* 1319.3954, found *m/e* 1319.3916.

Bilayer-Clamp Experiments. Alamethicin was obtained from Sigma and was not further purified. All electrolytes were analytical grade or better. The apparatus and general procedures for single-channel recording and analysis have been reported.¹² "Macroscopic" ion currents were recorded following addition of the compound, using PCLAMP 6.0 (Axon Instruments) software to generate applied potential functions and to record the current–time responses. Averaging of current–time records to give current–voltage response curves was carried out with Clampfit (Axon Instruments).

Vesicle Experiments. The general procedures for vesicle preparation and pH-stat titration have been previously reported.¹⁷ Compound **1** was dissolved in methanol (5.0 mM) and was directly added to the vesicle suspension to initiate transport. All experiments gave good (*r*² > 0.98) fits to a first-order expression for consumption of titrant as a function of time for the period of the experiment where the pH-stat controlled the pH. Rate data for 21 μM **1** and 0.02 M alkali metal sulfates (rate × 10¹⁰ mol of H⁺ s⁻¹; uncertainty of ±10%): Li⁺, 0.5; Na⁺, 1.4; K⁺, 2.0; Rb⁺, 14; Cs⁺, 3.4.

Acknowledgment. The continuing support of the Natural Sciences and Engineering Research Council of Canada and of the University of Victoria is gratefully acknowledged.

Supporting Information Available: ¹H and ¹³C NMR spectra of **1** (2 pages). See any current masthead page for ordering information and Web access instructions.

JA972648Q